Atom optics in the time domain

M. Arndt, P. Szriftgiser, and J. Dalibard
Laboratoire Kastler Brossel, 24 rue Lhomond, F-75231 Paris Cedex 05, France

A. M. Steane
Clarendon Laboratory, Parks Road, Oxford OX1 3PU, England
(Received 2 November 1995)

Atom-optics experiments are presented using a time-modulated evanescent light wave as an atomic mirror in the trampoline configuration, i.e., perpendicular to the direction of the atomic free fall. This modulated mirror is used to accelerate cesium atoms, to focus their trajectories, and to apply a ''multiple lens'' to separately focus different velocity classes of atoms originating from a point source. We form images of a simple two-slit object to show the resolution of the device. The experiments are modelled by a general treatment analogous to classical ray optics. [S1050-2947(96)08705-7]

PACS number(s): 03.75.Be, 32.80.Pj, 42.50.Vk

I. INTRODUCTION

The manipulation of the external degrees of freedom of atoms has attracted much interest during the last few years since powerful techniques such as laser cooling have become available. Today's experiments are typically in a regime where a classical analysis in terms of atomic trajectories is sufficient in some part of the experiment and where a quantum description is required in another region [1]. The present paper reports on a simple classical model and several experiments concerning the controlled manipulation and measurement of position and momentum of laser cooled atoms using a mirror formed by a time-modulated evanescent light field. This type of atom mirror has the advantage that it can be tailored without any major effort to interact with the atoms over a wide range of time and distance scales. For slow modulation the atoms follow classical trajectories during their reflection, while for fast modulation a full quantum description is necessary [2]. This is the temporal equivalent of the transition between ray optics and wave optics for light.

For atom optics one wants to have optical components such as precisely shaped lenses, apertures, prisms, and mirrors of selectable orientation and position. Matter optics, with electrons, neutrons, and recently also atoms, has for the most part taken its inspiration from light optics, so that one envisages the relevant wave moving through a series of ''optical components'' fixed in space. However, one can influence the atomic (or electron, or neutron) motion not only using optical elements with a spatially varying structure (such as lenses) but also in a very general manner by using devices that are made to undergo a prescribed time variation. Sideband generation is a simple example and nowadays a standard application (using electro-optic modulators) of this idea in optics. It was realized for neutrons by Felber and his colleagues [3] using a resonant mode of vibration of a crystal on which neutrons were reflected. Phase modulation for atom waves was realized by Steane *et al.* [4] using a modulated atomic mirror similiar to that which will be at the heart of the experiments to be described in this paper.

The manipulation made possible by a time-modulated mirror controls the atomic motion along the direction z normal to the mirror surface, rather than in the transverse direction x as for most standard optical instruments. For example, a standard lens will, in general, form the image of a point (x_i,z_i) at a point (x_f,z_f). All the rays emerging from (x_i,z_i) arrive at (x_f,z_f), no matter what their initial angle of inclination to the z axis. In our case, we form the image of an initial event (z_i,t_i) at a final event (z_f,t_f). All rays leaving the initial event arrive at the final event, no matter what their initial velocity along the z direction.

Fast optical components are needed in order to manipulate the atoms that typically have short interaction times with the modulating device. While it is difficult to get massive material objects, such as a mirror substrate, to move fast enough (at a frequency of about 1 MHz) (see, however, [3,5–7]) one can circumvent this problem by using light fields to produce all the optical components. These can easily be made to vary rapidly in time.

The purpose of this article is to point out some general insights into the manipulation of atoms using time-dependent fields and, in particular, evanescent fields [8]. In Sec. II we start out with a derivation of the requirements that have to be fulfilled by a moving mirror in order to represent the equivalent of an atom lens in the time domain. The treatment remains classical and one-dimensional in this section and leads to imaging matrices known from standard optics that can be simplified using a paraxial approximation. The equations are then generalized to include gravity and are analyzed for some sample cases. In our experiment the reflecting mirror potential is generated using an evanescent light field; in order for the matrix treatment to be applicable to this situation, the exponential shape of the light potential has to be taken into account. This is done in Sec. III. Section IV describes the experimental setup, while Sec. V presents the realization of a moving mirror employed to play tennis with atoms, to image a double slit in the time domain, and to split an atomic beam into a choosable number of resultant beams sorted according to their velocity.

II. MOVING MIRROR

A. Imaging of particles with a moving mirror

We first consider the effect of a mirror moving at constant velocity, without specifying the exact nature of the experi-

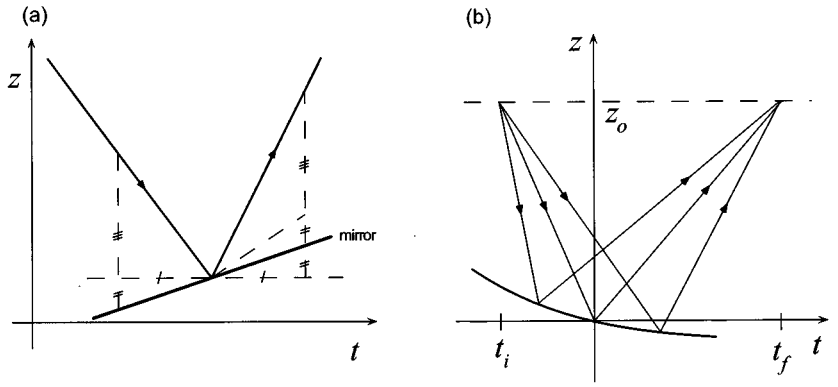

FIG. 1. (a) Reflection of a classical particle on a moving mirror. (b) Imaging of a pulse using an accelerating mirror. Particles emitted from an initial position z_0 at time t_i are reflected on the accelerating mirror. This gives them the velocity change necessary to compensate for the spreading, causing all the particles to come together again at z_0 at time t_f.

mental device that will be discussed in Sec. IV. While the effect of a stationary mirror is just to invert the sign of the momentum of the reflected particle ($v_f=-v_i$), a potential barrier moving at constant speed v_m can impart an additional momentum kick to the arriving atoms as a tennis racket does to an incoming tennis ball. After the reflection, the particle has the velocity

$$v_f=-v_i+2v_m. \tag{1}$$

This is illustrated in Fig. 1(a). Regarding the particle trajectory as a ray, we see that the moving mirror can map a ray striking its surface onto a ray departing at any angle in space-time by appropriately choosing the velocity of the mirror.

By allowing more general motions of the mirror surface, we can use it as a quite general ''optical element,'' which maps a group of incident rays onto whatever group of departing rays we require. For example, consider the case of ''imaging'' in space-time, illustrated in Fig. 1(b). We start with the assumption that atoms are emitted at position $z=z_i$ at time $t=t_i<0$. The atomic cloud spreads out due to its initial velocity distribution and thus arrives at any given position z with a spread of arrival times. However, by making the mirror surface move appropriately, we can arrange that the faster parts of the pulse are slowed down, while the slower parts are speeded up, with the result that the pulse is recompressed and the whole arrives at position z_f at a single time instant t_f. We define $t=0$ to be the time when the center of the pulse hits the mirror.

The appropriate motion of the mirror surface $z_m(t)$ is calculated as follows. We consider a particle having initial velocity v_i when arriving at the mirror surface at time t and we require this particle to travel after the reflection a distance $z_f-z_m(t)$ in time t_f-t. Therefore, it must leave the mirror surface at velocity v_f, which—according to Eq. (1)—imposes the following requirement for the mirror movement:

$$2\frac{dz_m}{dt}=\frac{z_f-z_m(t)}{t_f-t}+\frac{z_m(t)-z_i}{t-t_i}. \tag{2}$$

The solution for the time-dependent displacement of the reflecting surface can then be shown to be

$$z_m(t)=\frac{t_fz_i-t_iz_f}{t_f-t_i}\left(1-\sqrt{\frac{(t_f-t)(t_i-t)}{t_ft_i}}\right)+\frac{t(z_f-z_i)}{t_f-t_i}, \tag{3}$$

where we imposed the initial condition $z(0)=0$. Note that we have assumed the situation $|t_f|,|t_i|>|t|$ and $t_ft_i<0$, thus keeping the argument of the square root positive. The form of $z_m(t)$ is shown in Fig. 1(b), for the example case $t_f=-2t_i$, $z_i=z_f$. It is reminiscent of a ''concave mirror,'' although in our case the mirror surface is ''curved'' in space-time, not in space. Since a concave mirror has imaging properties similar to a lens, we will use the phrase ''temporal lens'' as well.

B. Paraxial and thin lens approximation

The formula (3) for $z_m(t)$ may be expanded in powers of t around $t=0$ to yield

$$z_m(t)=ut+\frac{1}{2}at^2, \tag{4}$$

where

$$u=\frac{1}{2}\left(\frac{z_f}{t_f}+\frac{z_i}{t_i}\right), \tag{5}$$

$$a=\frac{1}{4}\left(\frac{1}{t_f}-\frac{1}{t_i}\right)\left(\frac{z_f}{t_f}-\frac{z_i}{t_i}\right). \tag{6}$$

We will use this to construct a ''paraxial approximation'' for our time-dependent optical element. Let the ''optical axis'' be defined by the rays

$$z(t)=\begin{cases} tz_i/t_i & (t<0) \\ tz_f/t_f & (t>0). \end{cases} \tag{7}$$

We consider only rays close to this axis. A general paraxial ray starts at time $t=t_i$ from position $z(t_i)=z_i+dz_i$, with velocity $v(t_i)=z_i/t_i+dv_i$. By calculating the relevant particle trajectories, and keeping only terms to first order in dz_i, dv_i, one finds

$$\begin{pmatrix} dz_f \\ dv_f \end{pmatrix}=\begin{pmatrix} -t_f/t_i & 0 \\ 1/t_f-1/t_i & -t_i/t_f \end{pmatrix}\begin{pmatrix} dz_i \\ dv_i \end{pmatrix}, \tag{8}$$

where dz_f and dv_f give the final position and velocity of the ray, $z(t_f)=z_f+dz_f$, $v(t_f)=z_f/t_f+dv_f$. Regarding the positional distribution at time t_f as an image of the distribution at time t_i, Eq. (8) shows that the magnification is $|t_f/t_i|$. The transfer matrix in Eq. (8) can also be considered as a free

propagation for time t_i, followed by the effect of the moving mirror, followed by a free propagation for time t_f:

$$\begin{pmatrix} -t_f/t_i & 0 \\ (1/t_f-1/t_i) & -t_i/t_f \end{pmatrix} = -\begin{pmatrix} 1 & t_f \\ 0 & 1 \end{pmatrix}\begin{pmatrix} 1 & 0 \\ -1/f & 1 \end{pmatrix}\begin{pmatrix} 1 & -t_i \\ 0 & 1 \end{pmatrix}, \tag{9}$$

where the focal length of the system f is given by

$$\frac{1}{f}=\frac{1}{t_f}-\frac{1}{t_i}=\frac{2a}{u-z_i/t_i}. \tag{10}$$

Equation (10) is the temporal equivalent of the well known Gaussian formula for thin lenses $1/f=1/d_o+1/d_i$ where d_o, d_i are the distances between object (image) and lens. The minus sign in front of the lens matrix in Eq. (9) is caused by the fact that the velocity is reversed upon reflection. In all practical situations, $u>z_i/t_i$ since otherwise the mirror moves downward so fast that the rays never strike it. To find the position of the ray at some more general time $t\neq t_f$, one simply replaces t_f in the first matrix in Eq. (9) by t. The expression for the focal length f, Eq. (10), is the relative velocity of the mirror and the incident ray (evaluated at the reflection) divided by twice the acceleration of the mirror surface.

While the paraxial approximation implies that the velocity spread is small compared to the average velocity, we want to point out that in certain experiments—such as in the realization of a Fresnel lens (see Sec. V)—a further simplification is justified. This second approximation uses the fact that in the particular case $u=0$ the mirror coordinate varies only in second order as a function of time and can thus be assumed to be stationary [$z(t)=0$ for all times t, though $\dot{z}\neq 0$]. This assumption is the analogue of the ''thin lens approximation'' in light optics in which the lens has no extension along the direction of propagation of the rays.

C. Moving mirror and gravity

In the preceding section, we solved the problem of imaging a pulse in a one-dimensional space-time using a moving flat mirror, for the case in which the freely propagating rays are straight. We next consider the case of motion in a gravitational field. This will be important for the description of our experiments later in this article. We assume a constant gravitational acceleration of $-g$ in the z direction (that is, the z axis is directed vertically upward). An analysis similar to that above leads then to the solution

$$z_m(t)=\left(\frac{t_f z_i-t_i z_f}{t_f-t_i}-\frac{g}{2}t_f t_i\right)\left(1-\sqrt{\frac{(t_f-t)(t_i-t)}{t_f t_i}}\right) + \frac{t(z_f-z_i)}{t_f-t_i}+\frac{gt}{2}(t_f+t_i-t), \tag{11}$$

where the boundary condition $z_m(0)=0$ has been imposed. This gives the following paraxial solution for $z_m(t)$:

$$z_m(t)\simeq ut+\frac{1}{2}at^2, \tag{12}$$

where

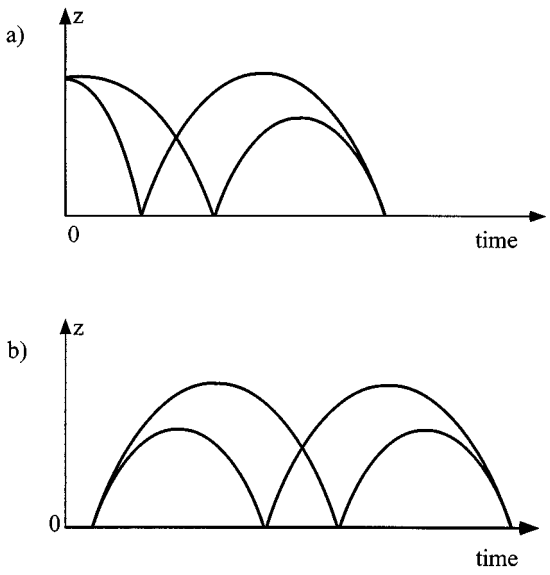

FIG. 2. Sample imaging situations. (a) An image is formed at the mirror surface of the atomic position distribution in a source such as a magnetic or magneto-optical trap positioned above the mirror. (b) An image is formed at the mirror surface of an object also at the mirror surface.

$$u=\frac{1}{2}\left(\frac{z_f}{t_f}+\frac{z_i}{t_i}\right)+g\left(\frac{t_f+t_i}{4}\right), \tag{13}$$

$$a=\frac{1}{4}\left(\frac{1}{t_f}-\frac{1}{t_i}\right)\left(\frac{z_f}{t_f}-\frac{z_i}{t_i}\right)-\frac{g}{8}\left(\frac{t_f}{t_i}+\frac{t_i}{t_f}+6\right), \tag{14}$$

where the optical axis is now defined by the rays

$$z(t)=\begin{cases} t(z_i/t_i+gt_i/2)-gt^2/2 & (t<0) \\ t(z_f/t_f+gt_f/2)-gt^2/2 & (t>0). \end{cases} \tag{15}$$

One finds that the effect of reflection of a paraxial ray on the mirror is once again given by Eqs. (8) and (9), where the focal length in the mirror matrix has now to be replaced by

$$f=\frac{u-z_i/t_i-gt_i/2}{2(a+g)}, \tag{16}$$

which is twice the relative acceleration of the ray and mirror surface divided by their relative velocity.

Two simple examples will give a more intuitive understanding of imaging with the moving mirror. We restrict ourselves to the case $u=0$ (so that the thin lens approximation applies) and consider first the imaging of a source such as a magneto-optical trap (MOT) positioned above the mirror. Atoms are released from the trap at $t=t_i$, and we choose to form an image just above the surface of the mirror, after one reflection at time $t_f=-2t_i$ and a free flight ($z_i\rightarrow z_f=0$). This is shown in Fig. 2(a). From Eq. (14) we derive the required mirror acceleration $a=-g/4$ and find $M=|t_f/t_i|=2$ as the magnification of the object in the image plane. This can be utilized to map the vertical spatial structure of the magneto optical trap above the moving mirror without being hindered by the velocity distribution of the launched particles.

The second example is the imaging of a time-dependent object at $z=0$. This is sketched in Fig. 2(b). The definition of the object is most conviently done using the modulated mirror, which can be made to reflect only a small packet of atoms out of the falling cloud. The object (temporal slit) is thus formed on the mirror at $z_i=0$ and, since the probe is also very close to the mirror, it is imaged to $z_f=0$ as well. Using this, we find the appropriate mirror acceleration $a=-g/2$ using the same method as before, which then yields an image with a magnification of $M=1$. In this particularly simple and symmetric situation, the prediction within the paraxial approximation is actually identical to the exact solution of the equations of motion.

III. EXPONENTIAL POTENTIAL

In our experiments, we used an evanescent light field propagating along the surface of a piece of glass to act as a mirror for incident cesium atoms [9–17]. For such a field, the light intensity decreases exponentially in the direction normal to the glass surface. The light field produces a repulsive potential for atoms in the ground state through the light shift (ac Stark shift) of the ground state energy level. The potential $V(z,t)$ for the atom takes the form [8,9]

$$V(z,t)=\frac{\hbar\Omega^2(z=0,t)}{4\delta}e^{-2\kappa z}, \tag{17}$$

where z is the distance from the glass surface and Ω is the Rabi frequency of the interaction between the light and the atom. Ω^2 is proportional to the light intensity, which depends on both z and time t. With $\delta=\omega_L-\omega_A$, we designate the detuning between the light frequency ω_L and the atomic resonance frequency ω_A.

To create a moving mirror, we require that the mirror potential $V(z,t)$ move in the z direction. This can be done, for example, by moving the glass surface, which would move the origin of z in Eq. (17). This is not convenient in practice. However, the exponential function has the special property that a change in its amplitude is equivalent to a displacement of the function along the z axis. Therefore, to cause the mirror to move, it is sufficient to cause the light intensity to vary in time, which can be done easily in practice. The time variation of V required to reproduce the effect of a moving mirror with trajectory $z_m(t)$ is

$$V(t)e^{-2\kappa z}\equiv V(0)e^{-2\kappa[z-z_m(t)]}. \tag{18}$$

To obtain the solution to the imaging problem in a gravitational field, one substitutes the expression for $z_m(t)$ into Eq. (18), which, for the particular case of paraxial motion, [Eq. (12)] takes the simple form

$$V(t)=V(0)e^{-2\kappa(ut+at^2/2)}. \tag{19}$$

We now discuss the limitations on the maximal mirror velocity and acceleration that arise from the facts that (i) there are some experimental limitations on the maximal and minimal values of $V(t)$ and (ii) this exponential potential is not a ''hard'' mirror and the reflection of atoms with incident velocity v_i takes a time of order

$$\tau_b\equiv\frac{1}{\kappa v_i}, \tag{20}$$

referred to as the ''bouncing time.''

We require τ_b to be small compared to the free flight time (of order v_i/g) between bounces, $\tau_b\ll|v_i/g|,|v_i+2v_m|/g$; otherwise, the motion cannot be divided into separate reflections and free flights as we are doing. For our experiments, $\tau_b\simeq1\ \mu$s, while the free flights last several tens of milliseconds, so the condition is well satisfied. The bouncing time also limits the maximum acceleration of the mirror surface, since we require that the change of mirror velocity $a\tau_b$ during the time spent by a given atom in the exponential potential is small compared with a typical mirror velocity v_m. This condition requires $|a|\ll|v_m|/\tau_b$. For our experiments $|v_m|$ does not exceed ~1 cm/s, for reasons given in the next paragraph, so the limitation corresponds to $|a|\ll10^4g$. Since we use typically $a\sim g$, we work well within the range of this approximation. Neither of the requirements described so far represent intrinsic limits of the experimental technique; they merely circumscribe the degree to which the simple matrix methods we have presented can be used to calculate the atomic trajectories.

In practice the limitation of the available power gives an upper limit on the potential: $V(t)<V_{\max}$. On the other hand, we should not decrease $V(t)$ below a certain value $V_{\min}$, for which the atoms incident on the mirror will not be reflected at all, but will stick to the glass. This puts an upper bound on the time Δt during which the mirror can be moved continuously; considering, for instance, a mirror with constant velocity $u=v_m$ $(a=0)$, we get

$$\Delta t\leqslant\frac{1}{2\kappa v_m}\ln\frac{V_{\max}}{V_{\min}}. \tag{21}$$

Consider atoms arriving on the mirror at velocity v_i. In order to get the required output velocity $v_f=-v_i+2v_m$ for at least some fraction of the atoms, Δt should be much longer than the bouncing time τ_b of the atoms on the exponential potential. This implies

$$v_m\ll\frac{v_i}{2}\ln\frac{V_{\max}}{V_{\min}}. \tag{22}$$

In practice, $v_i\sim20$ cm/s and $V_{\max}/V_{\min}\sim2$ so that we are limited to $v_m\leqslant1$ cm/s.

The limit on Δt is quite severe. For $v_m=1$ cm/s and $1/\kappa=2\times10^{-5}$ cm, we find $\Delta t=6\ \mu$s. This poses a problem, because it means that the useful properties of the moving mirror are only available during a very short time. Fortunately, we can overcome this restriction by realizing the equivalent of a Fresnel lens. Whenever the mirror potential reaches the limiting value $V_{\min}$ (respectively $V_{\max}$), we multiply (respectively divide) this potential by $V_{\max}/V_{\min}$. After this, the potential $V(t)$ is varied continuously according to (19) until the next shift. The required mirror velocity, which is the essential feature for imaging in the thin lens approximation, can then be obtained over times much greater than Δt, except for $\delta(t)$-function spikes occurring at the multiplication (division) events. We will denote this repeated multiplying of $V(t)$ at the required instants by the notation

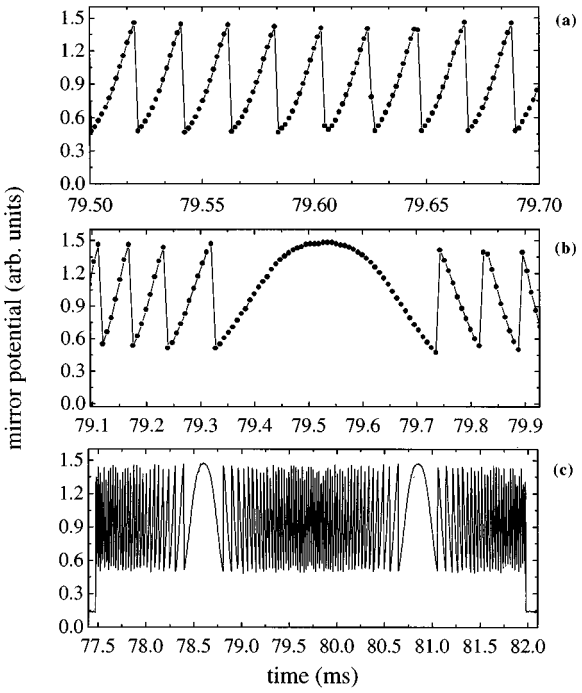

FIG. 3. Modulation schemes for the experiments. The curves show the power of the evanescent wave used in the experiment, as a function of time. The waveforms were generated by a programmable function generator. (a) Constant mirror velocity. (b) Constant mirror acceleration, lens experiment. (c) Multiple lenses. The temporal resolution in this figure is limited by the sampling time of a digital oscilloscope used to record the laser power. The function generator produced a new voltage level each microsecond.

$$[V(t)]_{\min}^{\max}. \tag{23}$$

The procedure is depicted in Fig. 3, which shows sample variations with time of the measured evanescent wave power in our experiment.

The abrupt shifts of the potential lead to a loss of resolution in the imaging properties of the system. To gain understanding of this, we have numerically solved the classical equations of motion and we find that the main effect of the shifts is that atoms whose trajectories are within the mirror potential when the latter changes abruptly are dispersed over a wide range of final velocities. In conditions comparable to those of our experiments, the numerical calculations predict that $\sim 80\%$ of the rays from a point source cross the image height within a time window of size $\sim \tau_b$.

Finally, the effects of diffraction enter in two ways. The finite total width in time of the optical elements gives rise to diffraction that limits the behavior near focal points of the trajectories. This is a standard limitation of optical systems, but our experimental resolution is not fine enough to detect it. The procedure of shifting the potential after each period Δt introduces a further wave-optical effect. The wave function of a reflected atom is divided into sections of duration Δt, which implies, by the properties of the Fourier transform (energy–time uncertainty relation), that the atom's kinetic energy is ill-defined, having a spread of order $\Delta E \sim \hbar/\Delta t$. This corresponds to a velocity spread $\Delta v \simeq \Delta E/M v_i$, where M is the atom's mass. Comparing this to the ''classical'' velocity change $2v_m$, we have $\Delta v/2v_m \simeq \hbar\kappa/M v_i$. In our experiments, $\hbar\kappa/M \simeq 2.5$ mm/s and $v_i \simeq 25$ cm/s, so the diffractive velocity spread is about 1% of the total velocity transfer. This is again too small to influence the experiments described in this paper.

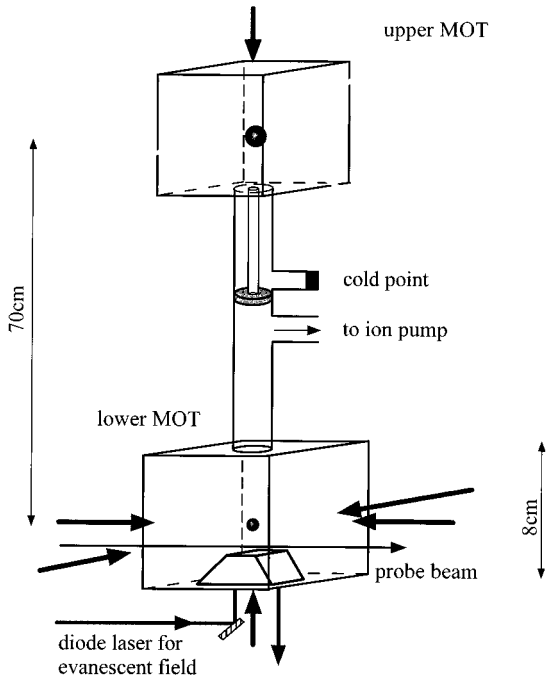

FIG. 4. Experimental setup (see text).

IV. EXPERIMENTAL SETUP

Our experiments used the same apparatus that we have described before [4]. Cesium atoms were allowed to fall in high vacuum onto an evanescent light field formed by total internal reflection of a laser beam inside a glass prism (Fig. 4).

The vacuum system consisted of two glass chambers, one 70 cm above the other, with a differential pumping tube connecting them. The upper chamber was first evacuated by an ion pump and a vapor of cesium was introduced. The pump was then switched off and the vapor pressure held at around 6×10^{-8} mbar by means of a cold finger. The lower chamber was evacuated by a continuously running 20 l/s ion pump, producing a background pressure less than 6×10^{-9} mbar. Atoms were loaded during 0.5 sec from the thermal vapor into a magneto-optical trap in the upper chamber, and then cooled and allowed to fall into the lower chamber, where they were captured in a second MOT. This produced a useful flux of atoms for the experiment (about 4×10^7 atoms per sec) while ensuring a very low partial pressure of cesium in the background gas in the lower chamber. Once the atoms were collected in the lower MOT, they were compressed by reducing the intensity per laser beam in the MOT to 0.5 mW/cm^2, and then cooled to 3.6 μK during 20 ms by switching off the magnetic quadrupole field and sweeping the laser detuning to $\delta = -9\Gamma$, where $\Gamma/2\pi = 5.2$ MHz is the full width at half maximum (FWHM) of the cesium atomic transition $g = 6S_{1/2}$, $F = 4 \rightarrow e = 6P_{3/2}$, $F = 5$.

Light for the experiment was produced by diode lasers. A grating-stabilized master laser was locked to the cesium line by saturated absorption spectroscopy and used to injection-lock two slaves, which provided light for both MOT's. When cooling the atoms, the laser detuning was changed by using a magnetic field coil wound around the saturated absorption cell to shift the frequency (by the Zeeman effect) of the saturated absorption feature to which the laser was servo-locked. A further laser stabilized to a Cs cell produced repumping light at the $F_g=3\rightarrow F_e=4$ frequency. We found that for the lower MOT to catch the slow (velocity ~ 3 m/s) atoms falling from the upper MOT, the intensity of the repumping light could be an order of magnitude lower than the intensity required for the upper MOT to capture atoms efficiently from the thermal vapor.

Light for the evanescent wave (EW) was provided by a high-power (200 mW) diode laser, injection-locked by a distributed Bragg reflector (DBR) diode laser. The high-power beam passed through an acousto-optic modulator (AOM) followed by a pair of elliptical apertures to remove stray light in the wings of the spatial profile. The polarization was adjusted using waveplates, and the beam passed into a fused silica prism inside the vacuum chamber, where it underwent total internal reflection at an angle of incidence $\theta=58°\pm 2°$. The polarization was set to be linear in the plane of reflection, which optimized the number of atoms reflected. Under these conditions the decay length of the evanescent wave is calculated to be

$$\frac{1}{\kappa}=\frac{\lambda}{2\pi\sqrt{n^2\sin^2\theta-1}} \tag{24}$$

$$=(0.19\pm 0.01)\ \mu\text{m}, \tag{25}$$

where $\lambda=852.1$ nm is the laser wavelength in vacuum, $n=1.452$ is the refractive index of fused silica at this wavelength. The uncertainty in κ arises mostly from the uncertainty in θ. We can deduce κ more accurately from our experiments, described below.

The Gaussian laser beam was focused to a spot size ($1/e^2$ intensity radius) of 400 μm at the total internal reflection, and the beam's ellipticity was such that the illuminated spot on the glass surface was circular. We measured a power of 100 mW in the laser beam before it entered the vacuum system.

The frequency of the DBR laser, which sets the frequency of the evanescent wave, was servo-locked to a transmission peak of a 10 cm Fabry-Perot etalon. The chosen transmission peak was set to be between one and two GHz (it was varied for different experiments) above the $F_g=4\rightarrow F_e=5$ atomic transition.

To modulate the intensity of the evanescent wave, we turned the acousto-optic modulator on and off. When it was fully on, more than 90% of the transmitted light fell in the first diffracted order from the AOM, which was blocked by the pinholes, thus reducing the EW intensity to less than 10% of its maximum value. This reduction is sufficient to guarantee that no atom can bounce on the mirror. To vary the intensity in a more general way, we used the circuit shown in Fig. 5. An 80 MHz sine wave is produced by a voltage-controlled oscillator and passed to rf switch A (see Fig. 5).

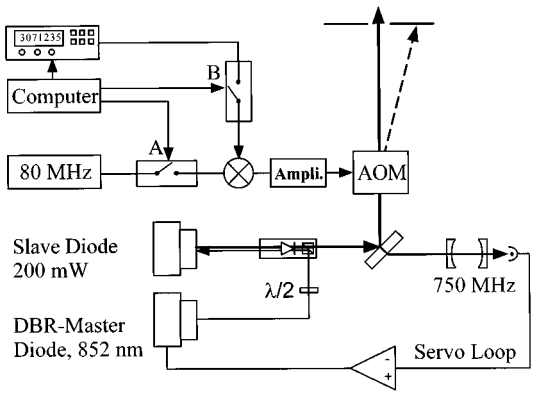

FIG. 5. Mixing circuit used to generate the modulation of the evanescent wave.

A general waveform $f(t)$ $(0\leqslant f(t)\leqslant 1)$, involving frequencies from dc up to a few MHz, is produced by a programmable function generator (Stanford Research Systems DS345), and sent to rf switch B. The outputs of the two switches are then amplified and passed to a mixer, the output of which is again amplified before being passed to the AOM. The AOM thus receives either nothing (both switches off), a pure 80 MHz sine wave (A on, B off), or an 80 MHz signal modulated by the programmed waveform $f(t)$ (both switches on). This causes the EW intensity be $I_{\max}$, $0.1I_{\max}$, or $I_{\max}g(t)$ [with $g(t)\equiv(1-0.9f(t)]$, respectively, assuming a linear response of the system. The switching time for the synthesiser-AOM system is of the order of 1 μs. This is of the order of the bouncing time τ_b of the atoms and well below the required time $\Delta t\geqslant 6$ μs during which the mirror position is continuously varied. Therefore, this finite switching time should not introduce significant deviations of the signal from the predictions obtained for an infinitely short multiplication or division time of $V(t)$ by the factor $V_{\max}/V_{\min}$. This was confirmed by including the experimental switching time in the numerical calculations.

The evanescent wave ''mirror for atoms'' is positioned ~ 3.3 mm below the center of the lower MOT. It therefore takes the freely falling atoms a time $T\simeq 26$ ms to reach the mirror surface. In general, our experimental procedure was to manipulate the mirror so as to produce a sequence of optical elements centered at times T and $3T$. These are the times at which the center of the cloud of atoms arrives at the mirror surface. After the third bounce the atoms are detected at $t\simeq 5T$ by switching on a probe laser beam positioned at variable height H above the surface of the mirror. The probe beam has a truncated Gaussian profile having a total width 200 μm. This width implies a temporal resolution of 0.8 ms for the detection of atomic arrival times in the probe. The probe beam is modulated in frequency at 56 kHz, and made near resonant with the $F_g=4\rightarrow F_e=5$ atomic transtion. Its absorption by the atoms is detected by a photodiode and lock-in amplifier. This time-of-flight signal gives information on the vertical distribution of the atoms after their interactions with the time-dependent mirror. Data were accumulated over a period of several minutes by repeating the experimental cycle.

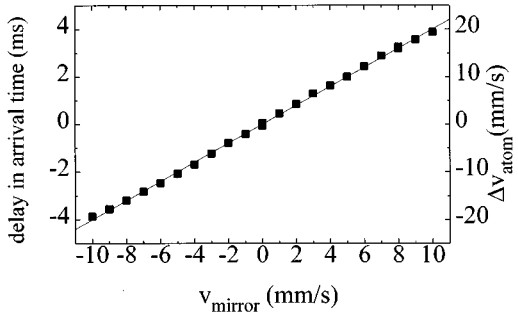

FIG. 6. Velocity change of atoms reflected from a moving mirror. Each data point represents an experiment in which the evanescent wave power varied exponentially with time, giving rise to a given constant mirror velocity. The simple law $v_f - v_i = 2v_m$ is thus verified.

V. EXPERIMENTAL RESULTS

A. Acceleration of atoms using a moving mirror

Our first experiment with the moving mirror was to produce a constant velocity v_m of the mirror surface, and thus impart a velocity kick to the bouncing atoms in close analogy with the action of a tennis racket. To produce the constant velocity of the mirror, we program the function generator to produce an AOM output of $I_{\max} g(t)$ with

$$g(t) = [e^{\beta t}]_{\min}^{1}, \tag{26}$$

where the square brackets denote the action of repeated rescaling described at the end of Sec. III [Fig. 3(a)]. In the experiments the ratio 1/min was typically 2. The mirror was pulsed ''on'' for two short pulses of duration 1 ms and 0.8 ms, separated by 53 ms, to select a small range of atomic velocities. In a calibration experiment, the the mirror was kept at constant intensity ($v_m = 0$) and the atomic time-of-flight (TOF) curve was recorded. Then the experiment was repeated using a modulated mirror in the second pulse, and the shift in arrival time of the atoms in the probe allowed their velocity change to be deduced. Figure 6 shows the observed velocity change of the reflected atoms, as a function of mirror velocity $v_m = \beta/2\kappa$. We obtain a linear dependence as expected, and if we assume the ''mirror law'' $v_f - v_i = 2v_m$, the data allow us to deduce the value $\kappa^{-1} = 0.193 \pm 0.004$ μm, in agreement with the expectation described in Sec. IV.

The pulse arriving in the probe laser beam 53 ms after the second mirror pulse had a temporal width of 1.3 ms if the second pulse was unmodulated. This is consistent with expectations when the initial pulse width (1 ms), probe beam diameter, and vertical heating due to scattered photons are taken into account: The probe beam had a width of about 200 μm, which gives rives to a TOF width of 0.7 ms for atomic velocities of 25 cm/s as used in the experiment. Photon scattering has to be considered as well. At a detuning of 2 GHz for the tennis experiments we expect about 0.26 scattered photons per atom and bounce. There are two bounces before the probing so that on average every second atom has a chance to absorb a single photon from the evanescent wave. The recoil-induced velocity change amounts to 1.4% of the incident atomic speed and gives rise to a maximum variation

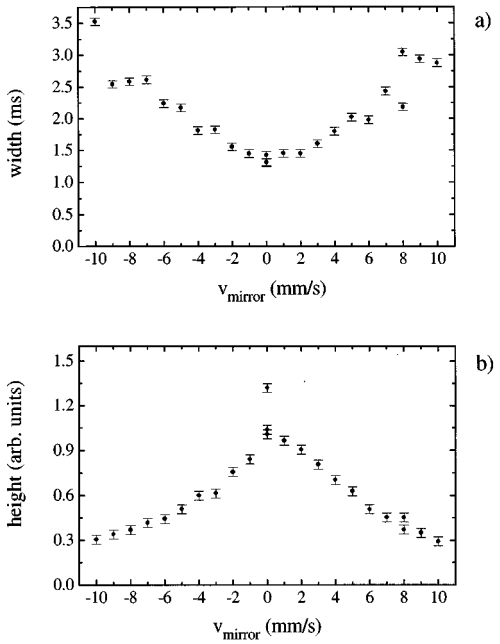

FIG. 7. (a) Velocity spread (FWHM) of atoms after reflection on a moving mirror, and (b) corresponding peak height of the time-of-flight signal, as a function of mirror velocity. These results demonstrate the imperfections of the experimental setup. The major imperfection is believed to be a nonlinear response of the acousto-optic modulator used to vary the evanescent wave power, rather than the intrinsic limitations of the method.

of 1.4 ms in the time of flight after two bounces. Neither of these three contributions (initial pulse width, probe diameter, number of absorbed photons) depends on the intensity of the evanescent wave [10,11].

However, we find that the TOF signal depends on the properties of the modulated mirror. When the mirror velocity is increased, the width of the atomic velocity distribution increases [Fig. 7(a)], while its height decreases [Fig. 7(b)]. The area of the velocity distribution also slightly decreases (by less than 50 %) between $v_m = 0$ mm/s and $v_m = 10$ mm/s. The spreading is much larger than that predicted by numerical calculations for an evanescent wave power proportional to $g(t)$ as given by Eq. (26). We found that nonlinearities in the response of our acousto-optic modulator could, in principle, be sufficient to account for this effect, since they lead to different effective accelerations at different times. The experimental response of the AOM is given in Fig. 8. A deviation from the calculated curve is noticeable when the transmitted light has a high intensity, i.e., in the first 20% of the time sequence. During this period, the effective velocity of the mirror can thus be reduced by a factor of up to three compared to the expected value. The corresponding asymmetric broadening of the TOF signal is increased when v_m increases. The contribution of these nonlinearities could be compensated for in future work by taking into account the response function when generating the synthesized function $f(t)$. As mentioned in Sec. III, there is another loss and broadening mechanism related to the fact that there are finite switching times between the exponentials during which the atoms undergo a large acceleration of inverse sign. This effect is nonnegligible at mirror speeds above $v_m = 1$ cm/s but

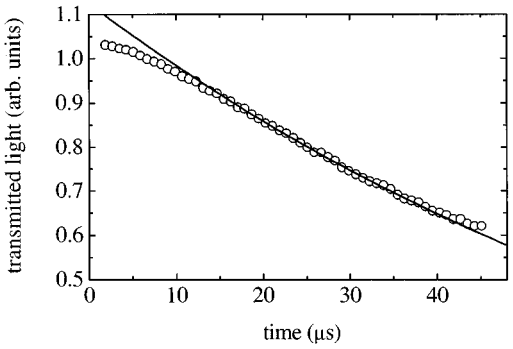

FIG. 8. Response of the acousto-optic modulator. The points show the measured evanescent wave power as a function of time in a sample experiment, while the line is the variation required to produce a constant v_m.

simulations show that it should be still too small to explain Fig. 7. Also, the slightly decelerating influence of the Van der Waals force is much too small to come into play.

B. Imaging with a time lens

We demonstrate imaging by the time sequence shown in Fig. 9 [cf. Fig. 2(b)]. Two short pulses (each of duration 0.4 ms) of the EW intensity centered around time $t=T$ produce an ''object,'' that is, a distribution of times of reflection on the mirror, since only atoms arriving when the EW is on are reflected. We then cause the mirror to act as a lens centered around $t=3T$, with the acceleration chosen so as to form an image at the height H of the probe beam (0.5 mm), centered at $t=(4+\sqrt{1-2H/gT^2})T=4.999T$. We used $T=26.5$ ms.

The function generator is programmed to produce $f(t)$ such that the evanescent wave intensity varies as $I_{\max}g(t)$, where

$$g(t)=[e^{\kappa a t^2}]^1_{\min}, \tag{27}$$

with $a=-g/2$.

Figure 10 shows the observed time-of-flight signals with the mirror stationary during the second bounce and with the moving mirror acting as a lens. We find that the lens enables us to form a true image of the two-peaked object. A series of measurements using objects of different spacing confirmed the expected 1:1 magnification within 10%. The resolution

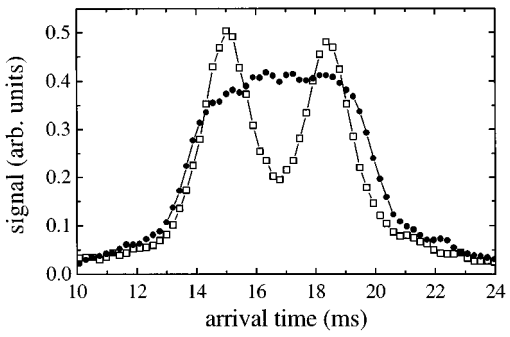

FIG. 10. Time-of-flight signals demonstrating imaging. The curves show the absorption of the probe beam as a function of time for an unmodulated mirror (●) and a mirror modulated so as to produce a temporal lens (□). When the lens is used, the image of the object—consisting of two pulses separated by 3 ms—appears.

depended on the total duration of the lens, becoming worse as the duration was increased (the duration of our temporal lens corresponds to the diameter of a familiar spatial lens). This implies that the resolution was limited by the nonlinear response mentioned in the preceding section rather than the finite width of the probe. For a lens of total duration 5 ms, the two peaks were just resolved when they were separated by 1.3 ms. We use the criterion that the peaks are resolved when a local minimum appears between them.

We can generate the atom optical equivalent of Billet's split lens [18] by programming the mirror to produce a set of lenses during the second bounce of the atomic cloud. The variation of the evanescent wave power for the case of two lenses is shown in Fig. 3(c). A total duration of 4.5 ms was divided into two sections, each containing a seperate lens programmed independently into the function generator. The expected motion of a selected atomic packet is shown in Fig. 11. The experimental TOF curve, measured at time $t=5T$, is shown in Fig. 12, where we varied the number of lenses in the second pulse from one [Fig. 12(b)] up to five [Fig. 12(f)], while keeping the total pulse duration constant. Another atom optical device — not demonstrated here but also easy to generate — would be a Fresnel biprism consisting of a mirror moving with positive velocity in the first half and with negative velocity in the second half of the second evanescent wave pulse (centered at time $t=3T$). Such multiple optical compenents could be used for coherent beam splitting, though the coherence times involved are longer than those of current atomic sources.

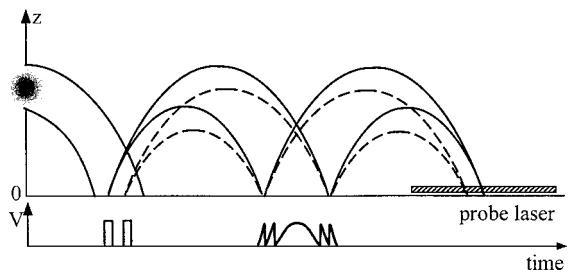

FIG. 9. Time sequence used to demonstrate imaging of a two-pulse object.

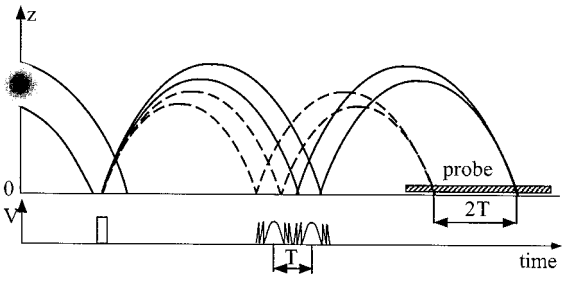

FIG. 11. Time sequence used to demonstrate the realization of Billet's split lens.

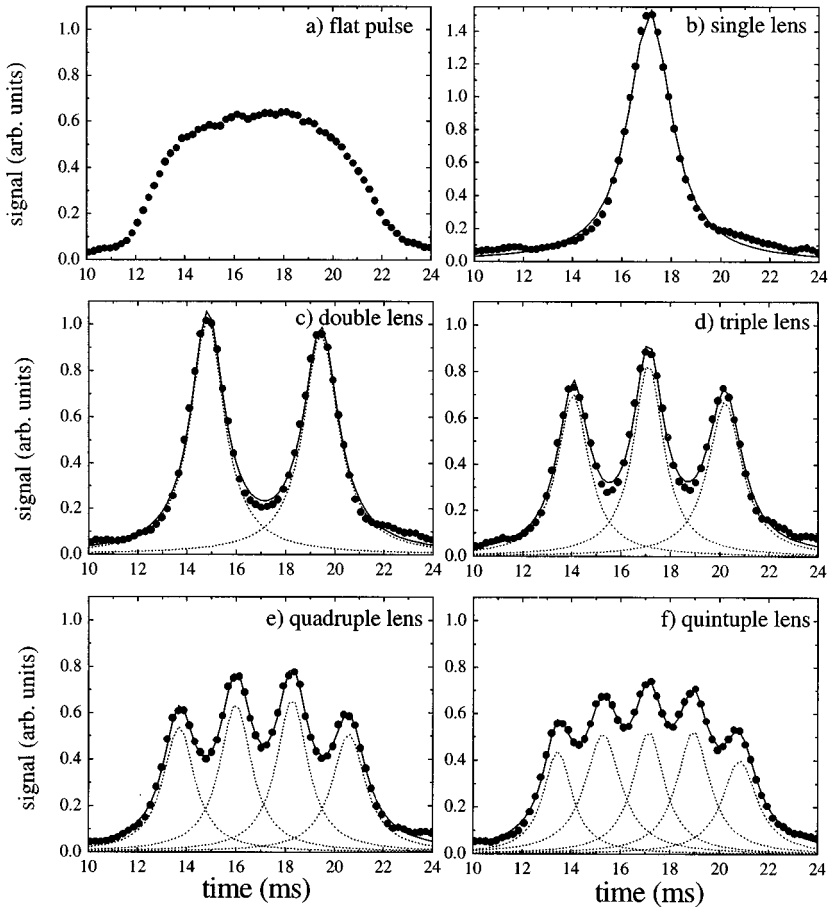

FIG. 12. (a) Multiple images of a point source, obtained by programming the mirror modulation so as to produce within the same time window — during the second bounce of the atoms — a sequence of lenses (a multiple lens). The total duration of the lens sequence was fixed at 4.5 ms, so individual lenses had a width in time equal to a fraction of this. (a) Unmodulated mirror, (b)–(f) multiple lens consisting of 1–5 lenses. The data can be fitted by summing together several Lorentzian curves having the same functional form as the image obtained with a single lens (b). The functions making such a fit are shown by the dotted curves. The roughly Lorentzian form is due in part to aberrations arising from the nonlinear response of the system, as discussed in the text, and in part to the truncated Gaussian profile of the probe laser beam.

VI. CONCLUSION

We have discussed the general idea of manipulating the motion of particles using time-dependent optical elements and shown than this can be a useful way of solving some of the basic technological problems in the field of atom optics, such as imaging. The moving mirror method solves the general problem of manipulating atomic motion along the direction normal to the mirror surface in the case of a pulsed source. It does not address the problem of imaging in the other (transverse) directions. However, for our experiments we do not, in fact, use a flat mirror, but one with a radius of curvature of 2 cm [11]. This means that if we were to drop the atoms from around 1 cm above the mirror, while also moving the mirror to focus the vertical motion, then a complete three-dimensional image of the atom source could be reconstructed.

We find that the potential produced by an evanescent light wave has two useful properties. First, it is produced by a light field and so can be varied rapidly (compared with magnetic fields and material objects). Second, its exponential form leads to a particularly simple analysis of the problem, since a change in amplitude is equivalent to a spatial translation of the potential. A third property, the short decay length of the potential, is useful in that it ensures that the optical element is thin and in that it reduces the heating due to scattered photons, but it also limits the time during which the potential can be changed continuously.

We have experimentally demonstrated three basic effects. The first is a simple velocity shift of an atomic beam by several times the recoil velocity associated with the light. The second is the imaging of a pulsed source. Numerical calculations show that the spatial resolution obtainable is of the order of the decay length of the evanescent wave, which is a fraction of a micrometer in our case, but the resolution in these first experiments was limited by imperfections in the apparatus. The third effect demonstrated is the formation of multiple images of a point source using a set of temporal lenses.

The modulated mirror can also serve as a diagnostic tool for the analysis of an atomic source. By allowing two bounces on lenses of different acceleration — corresponding to a strongly diverging lens followed by a converging one—a simple microscope could be constructed, allowing one to probe detailed structure in the source. Alternatively, a pair of short pulses can be used to select a small set of atomic trajectories, which corresponds to selecting atoms originating from a small range of initial velocity and position. By moving the center times of the pulses while repeating the experimental cycle, one can map the complete distribution of the atoms in the phase space of the vertical motion [(z,v_z) space]. We have built such a map, and deduced from it the temperature and density in our MOT. In principle, correlations between velocity and position can be observed this way, although we did not find any at the limited resolution of the measurements. By employing the methods of tomography [19–21], the complete initial Wigner function of the atoms could be deduced.

Finally, the modulated mirror can be used to investigate

the phenomenon of diffraction in time, that is, the spreading of the atomic trajectories implied by wave mechanics whenever the trajectories are restricted to a narrow range of arrival times at some position (here, the mirror surface). This will be explored in future work.

ACKNOWLEDGMENTS

We would like to acknowledge stimulating discussions and general encouragement from the E.N.S laser cooling group. M.A. acknowledges financial support as well by the CEC through a community training project and by the Alexander von Humboldt Foundation and wants to thank Claude Cohen-Tannoudji for his hospitality. A.M.S. was supported by the Royal Society. This work was partially supported by DRET, CNRS, Collège de France, and DRED. The Laboratoire Kastler Brossel is Unité de recherche de l'Ecole Normale Supérieure et de l'Université Pierre et Marie Curie, associée au CNRS.

[1] See, e.g., Appl. Phys. B **54** (1992) (Special issue on optics and interferometry with atoms); C. S. Adams, M. Sigel, and J. Mlynek, Phys. Rep. **240**, 143 (1994).
[2] C. Henkel, A. M. Steane, R. Kaiser, and J. Dalibard, J. Phys. (Paris) II **4**, 1877 (1994).
[3] J. Felber, Ph.D. thesis, Technischen Universität München, 1994.
[4] A. Steane, P. Szriftgiser, P. Desbiolles, and J. Dalibard, Phys. Rev. Lett. **74**, 4972 (1995).
[5] A. G. Klein, P. Prager, H. Wagenfield, P. J. Ellis, and T. M. Sabine, Appl. Phys. Lett. **10**, 293 (1967).
[6] W. A. Hamilton, A. G. Klein, G. I. Opat, and P. A. Timmins, Phys. Rev. Lett. **58**, 2770 (1987).
[7] E. Rasel *et al.*, *Proceedings of the Workshop on Waves and Particles in Light and Matter, Trani, 1992* (Plenum Press, New York, 1994), p. 429.
[8] R. J. Cook and R. K. Hill, Opt. Commun. **43**, 258 (1982).
[9] V. I. Balykin, V. S. Letokhov, Y. B. Ovchinnikov, and A. I. Sidorov, Pisma Zh. Éksp. Teor. Fiz **45**, 282 (1987) [JETP Lett. **45**, 353 (1987)]; Phys. Rev. Lett. **60**, 2137 (1988).
[10] M. A. Kasevich, D. S. Weiss, and S. Chu, Opt. Lett. **15**, 607 (1990).
[11] C. G. Aminoff, A. M. Steane, P. Bouyer, P. Desbiolles, J. Dalibard, and C. Cohen-Tannoudji, Phys. Rev. Lett. **71**, 3083 (1993).
[12] J. V. Hajnal, K. G. H. Baldwin, P. T. H. Fisk, H.-A. Bachor, and G. I. Opat, Opt. Commun. **73**, 331 (1989).
[13] T. Esslinger, M. Weidemüller, A. Hemmerich, and T. W. Hänsch, Opt. Lett. **18**, 450 (1993).
[14] S. Feron, J. Reinhardt, S. Le Boiteux, O. Gorceix, J. Baudon, M. Ducloy, J. Robert, Ch. Miniatura, S. Nic Chormiac, H. Haberland, and V. Lorent, Opt. Commun. **102**, 83 (1993).
[15] M. Christ, A. Scholz, M. Schiffer, R. Deutschmann, and W. Ertmer, Opt. Commun. **107**, 211 (1994).
[16] W. Seifert, R. Kaiser, A. Aspect, and J. Mlynek, Opt. Commun. **111**, 566 (1994).
[17] An atomic mirror with an exponential potential can also be achieved using a magnetic tape: T. M. Roach, H. Abele, M. G. Boshier, H. L. Grossman, K. P. Zetie, and E. A. Hinds, Phys. Rev. Lett. **75**, 629 (1995).
[18] M. Born and E. Wolf, *Principle of Optics*, 6th ed. (Pergamon Press, New York, 1980).
[19] K. Vogel and H. Risken, Phys. Rev. A **40**, 2847 (1989).
[20] M. G. Raymer, M. Beck, and D. F. McAlister, Phys. Rev. Lett. **72**, 1137 (1994).
[21] U. Janicke and M. Wilkens, J. Mod. Opt. **42** 2183 (1995).